**Natural Hazards
and Earth
System Sciences**

Clues to the identification of a seismogenic source from environmental effects: the case of the 1905 Calabria (Southern Italy) earthquake

A. Tertulliani and L. Cucci

Istituto Nazionale di Geofisica e Vulcanologia, Rome, Italy

Abstract. The 8 September 1905 Calabria (Southern Italy) earthquake belongs to a peculiar family of highly destructive (I_0=XI) seismic events, occurred at the dawning of the instrumental seismology, for which the location, geometry and size of the causative source are still substantially unconstrained. During the century elapsed since the earthquake, previous Authors identified three different epicenters that are more than 50 km apart and proposed magnitudes ranging from $M \leq 6.2$ to M=7.9. Even larger uncertainties were found when the geometry of the earthquake source was estimated. In this study, we constrain the magnitude, location and kinematics of the 1905 earthquake through the analysis of the remarkable environmental effects produced by the event (117 reviewed observations at 73 different localities throughout Calabria). The data used in our analysis include ground effects (landslides, rock falls and lateral spreads) and hydrological changes (streamflow variations, liquefaction, rise of water temperature and turbidity). To better define the magnitude of the event we use a number of empirical relations between seismic source parameters and distribution of ground effects and hydrological changes. In order to provide constraints to the location of the event and to the geometry of the source, we reproduce the coseismic static strain associated with different possible 1905 causative faults and compare its pattern to the documented streamflow changes. From the analysis of the seismically-induced environmental changes we find that: 1) the 1905 earthquake had a minimum magnitude M=6.7; 2) the event occurred in an offshore area west of the epicenters proposed by the historical seismic Catalogs; 3) it most likely occurred along a 100° N oriented normal fault with a left-lateral component, consistently with the seismotectonic setting of the area.

Correspondence to: A. Tertulliani
(tertul@ingv.it)

1 Introduction

The modern seismological networks currently use powerful technological tools that provide highest quality earthquake locations. On the contrary, we do not know with enough accuracy the epicentral location nor the source of a wide number of strong earthquakes occurred in the early decades of the past century. These earthquakes belong to a kind of 'shadow zone' that encloses all the events for which, for several reasons, we have poor seismological, macroseismic or geological data (seismic records, direct historical accounts, primary surface faulting etc). Therefore, in order to better characterize the source of these events we have to consider other kind of data such as earthquake-induced ground effects and hydrological changes, that have been known and were widely reported for centuries, but were progressively left aside with the advent of the fast-evolving instrumental seismology. Such environmental effects can be properly considered a footmark of the earthquake (e.g. Muir-Wood and King, 1993; Porfido et al., 2002; Pizzino et al., 2004), so they are potentially associated with its seismogenesis. The 8 September 1905 Central Calabria (Southern Italy) seismic event is a perfect candidate for this kind of studies.

In this study we want to support new evidence concerning the location and magnitude of the 1905 event, discriminating between three different epicentral solutions: A offshore westward, B inland and C offshore northward (Fig. 1 and Table 1). We will also provide new clues on the geometry of the event source, checking several individual faults associated with those locations. To these aims we will: 1) describe the remarkable dataset of environmental effects caused by the earthquake; 2) derive reliable magnitudes from the distribution of ground effects and hydrological changes; 3) use these magnitudes in empirical relations to deduce fault area and seismic slip of a number of potential sources at locations A, B, and C, and calculate the coseismic strain field associated
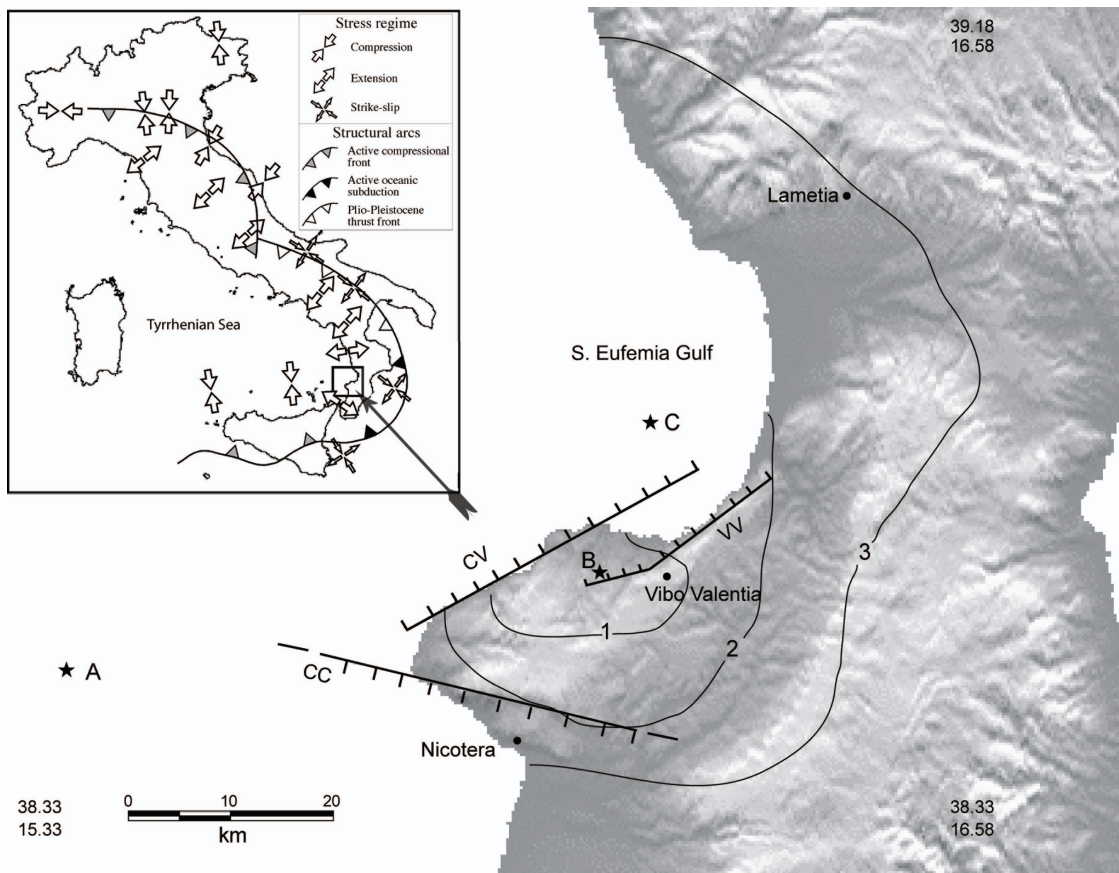
Fig. 1. Map of the area hit by the 8 September 1905 earthquake. Black stars indicate the three different epicentral locations investigated: A offshore westward (Michelini et al., 2006). B inland (Baratta, 1906; Mercalli, 1906; Boschi et al., 1995; CPTI Working Group, 2004). C offshore northward (Rizzo, 1907; Riuscetti and Shick, 1974; Martini and Scarpa, 1983; Mulargia et al., 1984; Postpischl, 1985; Westaway, 1992). CV (Capo Vaticano Fault), VV (Vibo Valentia Fault) and CC (Coccorino Fault) are three fault segments (hachures on the downthrown block) that are potentially associated with the event according to Piatanesi and Tinti (2002) (CV and VV) and Cucci and Tertulliani (2006) (CC). Black lines include: 1) highest level of destruction (intensity 9–10/10 MCS), 2) very heavy damage (intensity 8–9/9 MCS), 3) heavy damage (intensity 7–8/8 MCS). A grey arrow indicates the area in study. The inset shows a sketch of the structural arcs and of the regional stress regime in Italy (modified from Montone et al., 1999, 2004).

with those faults; 4) analyze which of the above cited sources better matches the environmental effects that we collected.

Our main purpose is to verify if it is possible to characterize an earthquake (in terms of magnitude, location, and geometry of the source) by using only the environmental effects produced by the quake itself.

2 Background on the 1905 earthquake

The earthquake struck in the early hours of 8 September a vast area of the Tyrrhenian side of the Calabria peninsula (Fig. 1), causing the death of 557 people and the heaviest damage (I_0=XI in CPTI Working Group, 2004) between the towns of Lametia and Nicotera.

The event produced a great number of effects on the environment (Fig. 2). Changes in the flow and in the temperature of rivers and springs were eyewitnessed over the entire

Calabria region, as well as diffuse ground cracking, landslides, liquefactions, and sparse light phenomena (e.g. Rizzo, 1907); all these environmental effects were observed soon after the earthquake. Moreover, a moderate tsunami was observed and recorded in the open sea and along the coastlines of Calabria and Sicily, and propagated northward in the Tyrrhenian Sea to large distances from the epicentral region (e.g. Boschi et al., 1995).

Among the highly destructive earthquakes that struck the Italian peninsula in the past century, the 8 September 1905 event is one of the most significant and one of the less understood at the same time. So far no convincing or unambiguous elements exist on the location and the geometry of the earthquake fault, nor on its magnitude. The first hypotheses on the event location were by coeval Authors who investigated the most damaged area in central-western Calabria; among them Baratta (1906) and Mercalli (1906) inferred an

Table 1. List of the environment effects observed following the 1905 earthquake.

Locality	Lat.	Lon.	Distance from epicenter A (km) Ref.[1]	Distance from epicenter B (km) Ref.[2,3]	Distance from epicenter C (km) Ref.[4,5,6,7,8]	Hydrological effects	Ground effects
Conidoni	38.698	16.035	50	2	13		DIS
Fitili	38.675	15.931	40	9	20		✓
Piscopio	38.661	16.113	56	7	16	INC	COH
San Leo	38.719	16.023	49	4	11		DIS
Stefanaconi	38.672	16.121	57	8	15		COH
Triparni	38.680	16.067	52	3	14		COH
Zungri	38.654	15.984	45	5	19		DIS
Parghelia	38.681	15.923	40	10	20		CRA, ✓
Aiello Calabro	39.116	16.166	80	50	35		DIS, CRA
Curinga	38.826	16.313	76	29	19	INC, LIQ	
Maierato	38.706	16.191	63	14	13	INC, LIQ, TUR	CRA
Martirano	39.080	16.248	84	48	33	INC, LIQ, TEM	COH
Bivona	38.709	16.103	56	7	10		✓
Cessaniti	38.663	16.026	49	2	17	✓	COH
Gizzeria	38.980	16.206	75	36	22	DEC	COH, CRA
Mileto	38.608	16.068	52	9	22	DEC	COH
Monteleone	38.675	16.102	55	6	14		✓
Caraffa	38.880	16.486	92	45	35		COH, CRA
Dinami	38.528	16.147	60	20	31	INC	COH
Filandari	38.615	16.030	49	7	22		COH
Galatro	38.459	16.109	59	26	38	INC	DIS
Montalto U.	39.405	16.158	104	81	67	INC, LIQ	
Ricadi	38.626	15.867	35	16	28		CRA
Rosarno	38.487	15.976	47	22	37	INC, LIQ	
Rose	39.398	16.288	110	83	68	DEC	
S. Gregorio	38.643	16.104	55	7	18		COH
Sant'Anna	38.322	15.887	51	42	57		COH
Seminara	38.335	15.871	48	41	56	INC, LIQ	SPR
Tropea	38.674	15.898	38	12	22		CRA
Belmonte C.	39.160	16.079	79	53	40		COH, SPR, CRA
Cortale	38.838	16.411	85	37	27	INC	SPR, CRA
Feroleto A.	38.962	16.388	88	44	31	LIQ	
Gerocarne	38.587	16.219	65	19	26		SPR
Girifalco	38.822	16.425	86	38	28	TUR	
Lago	39.168	16.147	83	55	40	INC	COH
Nicotera	38.551	15.938	42	17	31	INC, LIQ	
Polistena	38.406	16.076	59	31	44	INC	
Rombiolo	38.596	16.004	47	10	24	DEC, TUR	
San Floro	38.837	16.519	94	46	37	INC	COH, SPR
San Martino	39.489	16.108	109	89	75		SPR
Scigliano	39.127	16.306	91	55	40	✓	
Cetraro	39.516	15.941	106	93	80	INC, TEM, TUR	
Cir`	39.380	17.064	161	118	105		CRA
Cleto	39.090	16.158	78	47	32	INC	CRA
Gagliato	38.676	16.462	86	37	34	INC	
Isca sullo Ionio	38.600	16.519	91	43	43	TEM	
Longobardi CS	39.208	16.077	82	59	45	DEC	
Longobardi VV	38.702	16.122	57	8	11	DEC, TUR	
Miglierina	38.947	16.471	92	47	35	DEC	
Mongiana	38.513	16.319	75	31	37	✓	
Orsomarso	39.799	15.909	134	124	112	TUR	
Reggio C.	38.108	15.647	60	72	87	TEM	
Sambiase	38.966	16.282	79	38	24	INC, TEM	
Tiriolo	38.947	16.509	97	51	39		DIS

Table 1. Continued.

Locality	Lat.	Lon.	Distance from epicenter A (km) Ref.[1]	Distance from epicenter B (km) Ref.[2,3]	Distance from epicenter C (km) Ref.[4,5,6,7,8]	Hydrological effects	Ground effects
Vallelonga	38.646	16.294	72	23	24	DEC, LIQ	
Vena Sup.	38.660	16.057	51	3	16		COH
Acri	39.490	16.386	124	95	80		CRA
Cassano Ionio	39.784	16.317	147	125	111	INC, TUR	
Marcellinara	38.928	16.494	95	49	37	INC, LIQ, TEM	COH
Santa Sofia	39.546	16.329	126	100	85	INC	CRA
Amaroni	38.792	16.446	87	38	30	INC, LIQ	
Amato	38.942	16.463	93	48	36		SPR
Belcastro	39.017	16.785	122	75	64	INC	
Bonifati	39.586	15.902	112	101	89	INC	
Centrache	38.728	16.430	84	35	30	INC	
Gasperina	38.739	16.508	91	41	36	INC	
Guardavalle	38.505	16.505	91	45	48	DEC	COH
Caulonia	38.381	16.409	87	47	54		DIS
Civita	39.827	16.313	151	129	115	INC	
Petilia P.	39.111	16.789	126	81	69	DEC, TUR	
Canna	40.094	16.504	185	162	148	INC	
Crucoli	39.424	17.003	159	117	104		COH
Petronà	16.758	16.758	121	75	63	INC	

For each locality the table shows the geographical coordinates. Columns 4 to 6 report the distance from the three most quoted epicenters associated with the event (epicenter A: 38.63 N–15.47 E; epicenter B: 38.68 N–16.03 E; epicenter C: 38.80 N–16.10 E) and the relative references (see also main text and Fig. 1). Symbols of the hydrological observations: INC increase of the streamflow; DEC decrease of the streamflow; TEM rise of water temperature; TUR turbid flow; LIQ liquefaction. The mere tick $\sqrt{}$ (reported in three localities) indicates unspecified variations of streamflow. Symbols of the ground effects: COH coherent slide; CRA crack; DIS disrupted slide; SPR lateral spread. The mere tick $\sqrt{}$ (reported in four localities) indicates unspecified type of landslide.

References for the three epicenters: [1] Michelini et al. (2006); [2] Boschi et al. (1995); [3] CPTI Working Group (2004); [4] Riuscetti and Schick (1974); [5] Martini and Scarpa (1983); [6] Mulargia et al. (1984); [7] Westaway (1992); [8] Postpischl (1985).

inland epicenter close to Vibo Valentia (location B in Fig. 1), while Rizzo (1907) suggested an offshore location in the Gulf of S. Eufemia (location C in Fig. 1), based also on the analysis of few seismic recordings. In the following decades, Riuscetti and Schick (1974) and Martini and Scarpa (1983) provided a similar offshore epicenter, although with different values of magnitude (M_s=7.0 and M_k=7.3, respectively). Different locations of the event were also reported in the catalogs of Italian historical seismicity, as Postpischl (1985) again located the earthquake offshore, close to location C, while CPTI Working Group (2004) moved it inland close to Vibo Valentia (location B). In more recent times Michelini et al. (2006) proposed, by means of probabilistic algorithms, a new hypocentral location about 30 km offshore to the west of Capo Vaticano (location A in Fig. 1).

As for the magnitude, the 1905 event has been considered as a moderate, a strong, and even a major earthquake. Indeed we can pass from Westaway (1992), who claimed a $M \leq 6.2$ for the event by comparing the 1 m tsunami height of the event to that (8–12 m) produced by the nearby 1908 earthquake, to M_s=6.8 suggested by Abe and Noguchi (1983) in their Catalog of revised magnitudes, to the value of M_s=7.9 calculated by Duda (1965). To complete the ref-

erence frame of the energy released by the 1905 event we cite Galli (2000), who calculated a minimum M=7.38 on the base of indications of liquefaction features. Further studies about the 1905 event were provided by Fantucci and Sorriso-Valvo (1999), who found earthquake-induced growth anomalies in trees through dendro-geomorphological analysis, and by Tinti et al. (2004), who associated to this event a tsunami intensity 3 (on a scale of 6 degrees) in the New Catalogue of Italian Tsunamis.

Uncertainties on the geometry and kinematics of the source of the 1905 earthquake are also remarkable. According to Riuscetti and Schick (1974) the event probably occurred on a subvertical thrust fault, whilst Mulargia et al. (1984) stressed that the occurrence of a tsunami wave implies large coseismic displacements and suggested a normal faulting mechanism for the event. Piatanesi and Tinti (2002) tried to model the tsunami waves but could not discriminate between the offshore Capo Vaticano Fault and the inland Vibo Valentia Fault (both NE-trending and NW-dipping, Fig. 1). Cucci and Tertulliani (2006) compared the set of geological, topographic and macroseismic data and found that the WNW-trending, SSW-dipping Coccorino normal fault (Fig. 1) is a candidate source of the earthquake.

3 The environmental effects of earthquakes

3.1 Ground effects

Moderate to strong earthquakes ($M > 5.0$) are capable to produce peculiar ground effects on the environment. Those coseismic effects can be primary, if permanent features (i.e. surface faulting) are directly produced by the earthquake, or secondary, if they are triggered by the ground motion (e.g. landslides, slope failures, liquefaction, cracks, etc.). The area affected by landslides or other ground failures is strongly dependent on the magnitude and on other critical factors such as the rupture fault distance or the epicentral distance (Keefer, 1984), the lithology and the slope steepness (Keefer, 2000). However, the distribution of ground effects on the territory is conditioned by many triggering factors in addition to the earthquake, as soil conditions, vegetation, rainfall, weathering, slope, water content, drainage (Kojima and Obayashi, 2006). Several statistical investigations found that, for different magnitudes, an upper threshold can be individuated for the distance epicenter/landslide. Strong earthquakes can trigger landslides over hundreds kilometres from the rupture fault or the epicenter (Keefer, 1984). However, most of secondary ground effects are common within 80-90 km from the epicenter (i.e. Harp and Jibson, 1996; Rodriguez et al., 1999), as observed also for several Italian earthquakes (Esposito et al., 2000; Prestininzi and Romeo, 2000; Porfido et al., 2002).

3.2 Hydrological changes

Hydrological changes associated with earthquakes have been observed since centuries. The interactions between earthquakes and hydrological processes include variations of streamflow, wells' level, liquefaction, and variations in the chemical characteristics of waters. Most of them are of coseismic nature, but their occurrence has been also observed prior or after a major event. Muir-Wood and King (1993), Esposito et al. (2000), Porfido et al. (2002) tried to infer, for historical earthquakes, some relationship between such disturbances and the earthquake characteristics (fault type, epicentral distance, intensity and magnitude). In particular, Muir-Wood and King (1993) found that hydrological changes would accompany major normal fault, showing increase in streamflow and spring rise; reverse faults, on the contrary, would show negligible or undetectable effects, whilst strike slip and oblique faults would generate a combination of responses. Recently, the spatial pattern of water level changes has been compared with simulated coseismic strain changes (Grecksch et al., 1999; Ge and Stover, 2000; Lee et al., 2002; Montgomery and Manga, 2003; Caporali et al., 2005). The area interested by contractional volumetric strain seems to be in good agreement with the water level rise and water excess in streamflows. Montgomery and Manga (2003) underlined that the response of aquifers is different when considering the
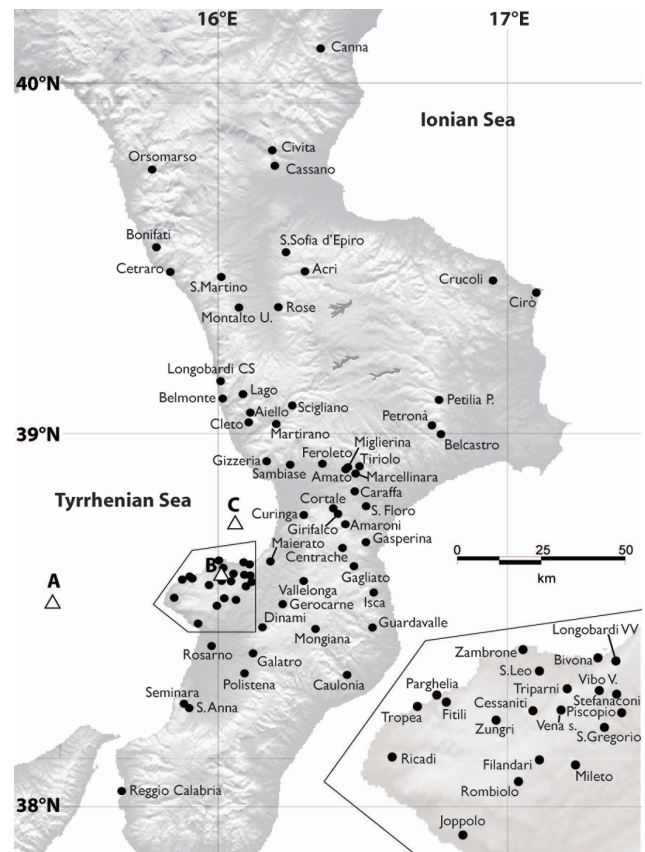

Fig. 2. General map of the environmental effects produced by the 8 September 1905 earthquake. Black dots indicate the 73 localities where one or more environmental effects were observed. The three alternative locations in study are indicated by triangles. The inset shows a blow-up of the area of Capo Vaticano.

near field or the far field, the transient or sustained response and the time scale over which a change occurs.

We include liquefaction in hydrological effects, considering that it can be one of the mechanisms that contributes to the increase in stream flow by means of the expulsion of water from compaction of unconsolidated deposits. The maximum distance to which liquefaction occurs is consistent with the maximum distance to which increase of streamflow has reported (Manga, 2001; Montgomery et al., 2003).

4 Environmental effects induced by the 1905 earthquake

4.1 Data collection

Our reference documents, both coeval and subsequent to the 1905 Calabrian earthquake, describe widespread environmental effects, observed in the aftermath of the event throughout the affected area (Baratta, 1906; Lais, 1906; Mercalli, 1906; Rizzo, 1907; Almagià, 1910; Montanari, 1940;
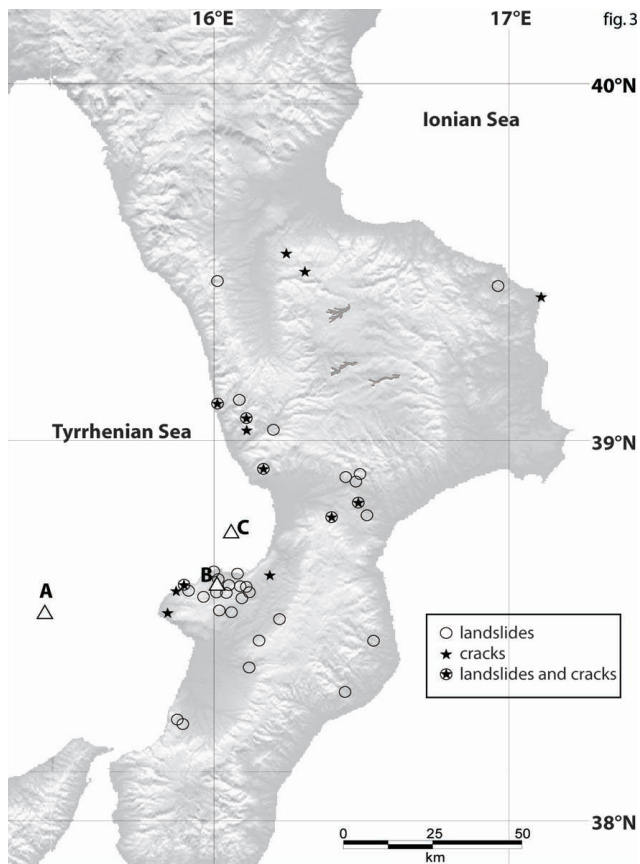
Fig. 3. Sites of ground effects. Triangles indicate the three locations in study A, B, and C.

Fig. 4. Sites of hydrological effects. Triangles indicate the three locations in study A, B, and C.

Chiodo et al., 1999; Fantucci and Sorriso-Valvo, 1999). After a careful revision of each quoted effect we stored a dataset of 117 deeply reviewed observations at 73 different localities (Fig. 2 and Table 1). The collection concerned two main groups of observations: ground effects (failures, landslides, cracks) and hydrological changes (flow variations, physical and chemical variations, liquefactions).

4.2 Ground effects

We collected useful data for forty-two localities where one or more ground failures (landslides, rock falls, lateral spreads in soil or simply cracks) occurred (Fig. 3 and Table 1). Unfortunately, we were unable to estimate the volume of the generated landslides, although we know from the chronicles that several of them were the main cause of damage and victims in some villages (i.e. Martirano, Ajello, Fitili, Parghelia; Fig. 2 and Table 1). Most of those landslides can be classified as coherent slides, few as disrupted slides and falls (sensu Keefer, 1984); occasionally the documents described reactivated landslides. In addition, chronicles reported many slope-parallel ground cracks, that can often be interpreted as incipient landslides. None of the recognized
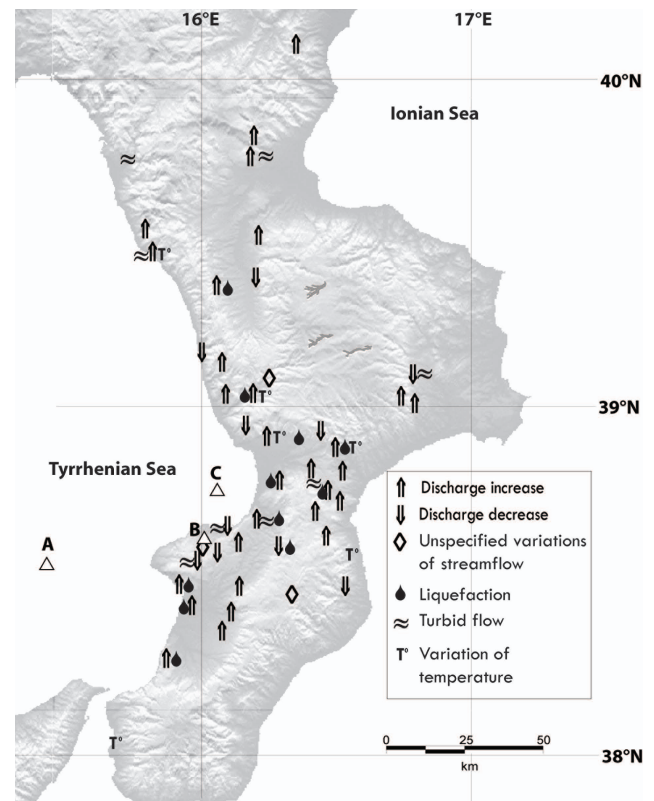
ground failures has been directly related to primary surface faulting (Mercalli, 1906; Galli and Bosi, 2002; Cucci and Tertulliani, 2006), even if the magnitude of the 1905 earthquake is around 7, so capable of breaking up through the surface. The 90% of cracks and landslides occurred within 60 km from the locations B and C, and within 90 km from location A (Fig. 3 and Table 1).

4.3 Hydrological changes

We collected forty-seven reports of localities throughout Calabria (Fig. 4 and Table 1) where one or more observations of hydrological changes occurred following the earthquake (Mercalli, 1906; Rizzo, 1907; Galli, 2000). Most of the data concerned excess flow in streams and springs; less frequently, a flow decrease or spring disappearance was reported. In some cases, we had notices of localities where the coeval accounts reported unspecific flow variations. These variations were sometimes accompanied by changes in the physical characteristics of the waters such as rise of their temperature and turbidity. The six localities where a temperature increase was reported fall into river basins with increase of flow. Liquefaction was observed in several localities, mostly where the same phenomenon was already noticed during past earthquakes.

Hydrological changes were observed up to 185, 162 and 148 km from epicentres A, B, and C, respectively (Fig. 4 and Table 1). As expected, hydrological changes occurred at longer distances than other environmental signatures. Indeed 90% of data was distributed within 140, 120, and 100 km from epicentres A, B, and C, respectively.

5 Magnitude of the 1905 event from environmental effects

In order to constrain the size of the earthquake on the basis of the above reported characteristics of the environmental effects, we used a number of empirical relations between seismic source parameters and distribution of ground effects and hydrological changes. In particular, in this section we evaluated the total area affected by seismically-induced landslides, or put in relation the maximum distance of each kind of earthquake-induced effect from the three alternative locations A, B, and C.

5.1 Magnitude derived from ground effects

We compared our data to the database of the pioneer work of Keefer (1984), who elaborated relations between magnitude and distribution of earthquake-induced landslides. The total area affected by landslides following the 1905 earthquake is ~6000 km^2: using the empirical relations we obtained a magnitude $M=6.7$ (Fig. 5). This is a particularly important value because the area affected by landslides usually shows a strong correlation with magnitude (Keefer, 1984). However, we want to stress that the $M=6.7$ estimate is a minimum value because of the possibility of an offshore epicenter, of the narrow shape of the Calabria peninsula, and because it is obtained on the upper-bound fit of the Keefer's data (Fig. 5).

Using the relation between earthquake magnitude and maximum epicentral distance of landslides, relative to the three inferred locations A, B, and C, we found mean values of magnitude (weighted means as a function of the number of observations) $M=6.71$, $M=6.44$ and $M=6.39$ for the three major categories of landslides (i.e. coherent slides, disrupted slides and lateral spreads) described by Keefer (1984) (Fig. 6).

5.2 Magnitude derived from hydrological effects

To derive a magnitude value from this environmental effect we referred to Montgomery and Manga (2003), who found that the maximum distance to which seismically-induced hydrological changes have been reported is related to the earthquake magnitude. In particular, these authors showed that the limiting distance to which liquefaction is observed also defines the upper limit to the envelope of reported streamflow responses to earthquakes. Starting from this key-point, we selected from Table 1 the maximum distance of the locality where concurrent increase of streamflow and liquefaction
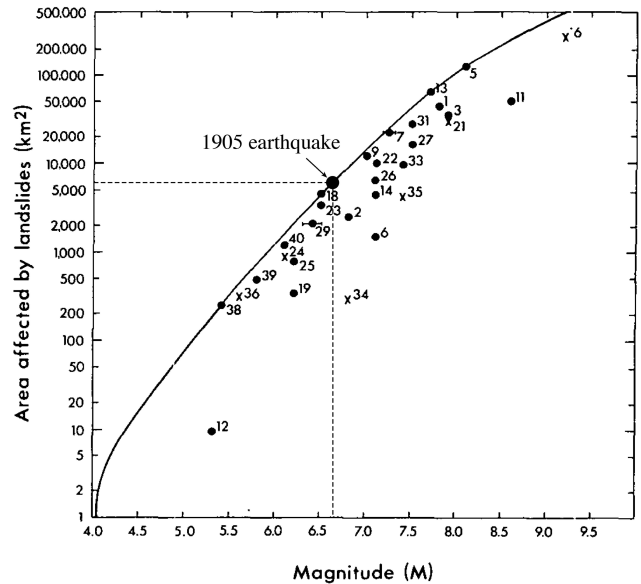

Fig. 5. Plot of the area affected by landslides (km^2) as a function of earthquake magnitude (after Keefer, 1984). Landslides following the 1905 event covered a total area of ~6000 km^2, which corresponds to a magnitude $M=6.7$.
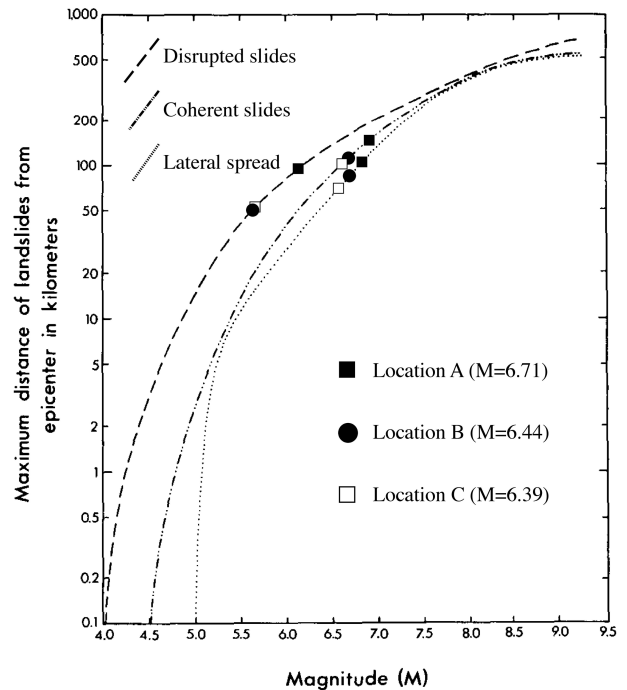

Fig. 6. Upper bound curves of the relation between earthquake magnitude and maximum distance from the epicenter of the landslide distribution (after Keefer, 1984). Mean values of magnitude $M=6.71$, $M=6.44$ and $M=6.39$ result from the intersection of the distances from the locations A, B, and C with the three major categories of landslide.
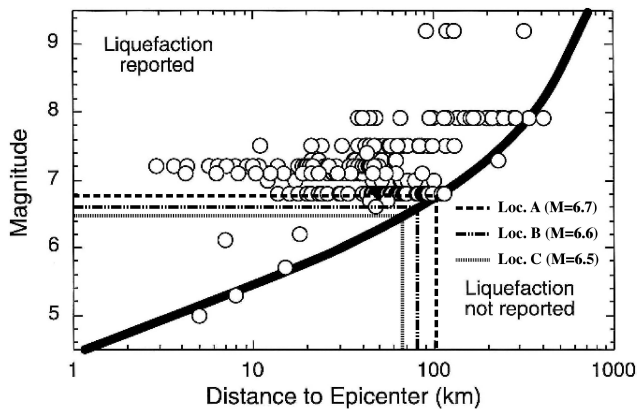
Fig. 7. Plot of the distance from epicenter versus earthquake magnitude for sites that exhibited seismically-induced streamflow response (after Montgomery and Manga, 2003). The solid line represents the empirical limit to the distance from the epicenter, beyond which liquefaction has been observed. Following the 1905 event, concurrent increase of streamflow and liquefaction was testified up to 104 km, 81 km and 67 km from the locations A, B, and C, respectively. This corresponds to M=6.7, M=6.6 and M=6.5 at the three potential epicenters.

was observed, and obtained M=6.7, M=6.6 and M=6.5 at the three potential epicenters A, B, and C, respectively (Fig. 7). We want to remark that also in this case these values are conservative, as they correspond to the minimum magnitude for an earthquake to produce liquefaction at a given distance, and also because liquefaction is not the exclusive cause of flow increasing.

5.3 Summary on the magnitudes derived from environmental effects

Magnitudes obtained both from ground and from hydrological effects are quite comparable. Averaging the values derived from the relations between magnitude, area affected by landslides, maximum distance of landslides and maximum distance of liquefaction, we obtain mean magnitudes M=6.70, M=6.58 and M=6.53 at the three locations A, B, and C, respectively. Such magnitudes are placed halfway between the extreme bounds proposed by Westaway (1992, $M \leq 6.2$) and Duda (1965, M_s=7.9) and fully comparable to the M_s=6.8 suggested by Abe and Noguchi (1983). In particular, we want to focus on the constant M=6.7 value obtained for location A from all the studied environmental effects. Therefore, for the 1905 event we define a minimum magnitude M=6.7 based on the empirical relations, and favour the epicenter A on the base of the consistency of the magnitudes obtained at this location.

6 Hydrological data and models of coseismic strain

In order to provide further constraints to the location and the geometry of the event source, we calculated the coseismic field of deformation produced by a number of individual sources potentially associated with the three locations investigated and compared it to the experimental data of streamflow changes. Our aim was to identify a preferred source, or alternatively to rule out some of the epicenters proposed by previous Authors.

We assumed that the observed streamflow variations are the hydrological response to coseismic strain changes (Muir-Wood and King, 1993). Several studies demonstrate that the polarities of calculated deformation are in agreement with those of the observed hydrological effects so that extensional strain produces a discharge fall and compressive strain a discharge rise, especially in the near field (Grecksch et al., 1999; Ge and Stover, 2000; Lee et al., 2002; Montgomery and Manga, 2003; Caporali et al., 2005).

However, in entering into a fall season of higher rainfall, the signature of stream flow associated with the earthquake can be perceptibly masked. For hydrological observations to be employed for this purpose it must be possible to show that, what is being observed is a consequence of seismic strain changes affecting crustal porosity. So we considered the rainfall in the days and weeks before and after the earthquake and found that the dry season prolonged until 20 September (Annali dell'Ufficio di Metereologia e Geodinamica Italiano, 1908). As the reports about stream flow changes referred to the first days following the event, we are confident that the hydrological signatures reflect coseismic strain.

Therefore, using the empirical relationships between magnitude and fault parameters by Wells and Coppersmith (1994) we deduced, from the mean magnitudes inferred through environmental effects, the fault area and the seismic slip of a number of generic sources at the three epicenters. Finally, we assigned a direction to each generic fault on the base of different evidences such as inversion of instrumental and intensity data (Boschi et al., 1995; Cucci and Tertulliani, 2006; Michelini et al., 2006), seismotectonic indications (Galli and Bosi, 2002; Piatanesi and Tinti, 2002; Neri et al., 2003; Tortorici et al., 2003), batymetric data and offshore profiles (Trincardi et al., 1987; Argnani and Trincardi, 1988; Gamberi and Marani, 2007).

At the end of this process we obtained five potential sources, that we summarize in Table 2 and briefly describe in the following:

– Western Offshore Fault (WO): it is associated with epicenter A, proposed as new hypocentral location of the 1905 event by Michelini et al. (2006).

– Macroseismic Fault North (MFN) and Macroseismic Fault South (MFS): they are derived from inversion of intensity data (Boxer code by Gasperini et al., 1999) and are associated with epicentral location B.

– Capo Vaticano Fault (CV): this fault has been used by Piatanesi and Tinti (2002) to model the tsunami waves generated by the earthquake. It is associated with epicenter C.

– Coccorino Fault (CC): this fault was selected it on the base of geological constraints (Tortorici et al., 2003; Cucci and Tertulliani, 2006), so that it is not strictly associated with any of the three epicentral locations.

For each source, we calculated the pattern of coseismic static strain expected for different geometries and styles of faulting. Calculations of the strain at the surface were made in an elastic halfspace with uniform isotropic elastic properties following Okada (1992) and using COULOMB 3.0 (Lin and Stein, 2004; Toda et al., 2005). The output of our calculations were plots of volumetric strain at the free surface on 60 individual faults (Fig. 8a–e and Table 3), obtained by crossing the five potential sources with two different dips (60° and 80°), two different depths of the top edge of the fault (0 and 5 km) and three different rakes (231° normal fault with right-lateral component/270° pure normal fault/309° normal fault with left-lateral component). We also tried the same calculations on the 500-m-deep surface, but the strain patterns were almost indistinguishable from the 0-m results.

To find out which of the above cited sources better matches the observed streamflow changes we selected only the solutions that showed: 1) within the distance of two fault-lengths, more than 50% of points with polarities of the observed hydrological effects in agreement with the expected deformation, and 2) percentage of consistent polarities at a distance of one fault-length higher than the percentage at two fault-lengths.

We comprised in the calculations only the localities up to a distance of two fault-lengths (in our case up to 46–58 km, see Table 2) from the center of the source, i.e. in the region where most significant hydrological changes should have occurred and where there is the highest chance to discriminate between models.

The results of this elaboration are depicted in Table 3; seven individual faults out of 60 satisfied both the conditions above described. A comparison between the seven preferred faults and the other solutions provided some interesting insights. Within two-faults distance, none of the solutions generated by the Capo Vaticano Fault (CV, Fig. 8e) showed a deformation pattern consistent with the observed one. The same poor fit was exhibited by the whole family of solutions with right-lateral component, independently from other parameters like the dip of the fault or the depth of its upper side. At one-fault distance, also the solutions associated with the Macroseismic Fault South (MFS, Fig. 8b) showed a low percentage of consistent polarities. Moreover, the good fit faults seemed to be greatly influenced by the rake (six solutions are with left-lateral component), partially by the position of the top edge of the fault (five solutions), and scarcely by the dip.

Table 2. List of the five potential sources.

Fault	Abbr.	Epicenter	Dimensions L×W (km)	Strike	M
Western Offshore fault	WO	A	29×17	100	6.7
Macroseismic Fault North	MFN	B	23×10	260	6.5
Macroseismic Fault South	MFS	B	23×10	80	6.5
Capo Vaticano fault	CV	C	24×10	245	6.5
Coccorino fault	CC	–	29×15	100	6.7

7 Discussion

Our dataset consisted of 117 observations at 73 different localities diffused over the Calabria territory. Data concerned a great number of notices of ground effects (landslides, rock falls and lateral spreads) and of hydrological changes (streamflow variations, liquefaction, rise of water temperature and turbidity). The analysis of these data provided i) sound evidence to assess the size of the 1905 earthquake, ii) several observations to reduce the uncertainties on its location, iii) some interesting clues to better define the geometry of the causative fault.

i) Evidence on magnitude: the empirical relations that we used to evaluate the size of the 1905 event from ground effects and hydrological changes concurred to individuate a magnitude between 6.5 and 7.0. We emphasize the M=6.7 value, which is calculated on the total area affected by landslides, a parameter that strongly correlates to the size of the event. We underline that this is a minimum value, because of the possibility of an offshore location, of the shape of the Calabria region, and of the limits of the Keefer's curve. Similarly, magnitudes between M=6.5 and M=6.7 (depending on the different location) were calculated by hydrological effects; we consider also these estimates as conservative. In summary, values of magnitude obtained from environmental effects were comparable and homogeneous. Taking into account the above described conservative constraints, we indicate M=6.7 as the most likely minimum magnitude of the 1905 event.

ii) Observations on location: we checked three potential target areas, identified as alternative epicenters by previous studies and indicated as A, B, and C in Fig. 1. From the empirical relations between magnitude and distribution of environmental effects we found that epicenter A is preferred because of the consistency of the magnitudes obtained at this location. As for the hydrological effects, we assumed that the streamflow variations are the hydrological response to coseismic strain changes (Muir-Wood and King, 1993), and compared the polarities of the observations (charge and
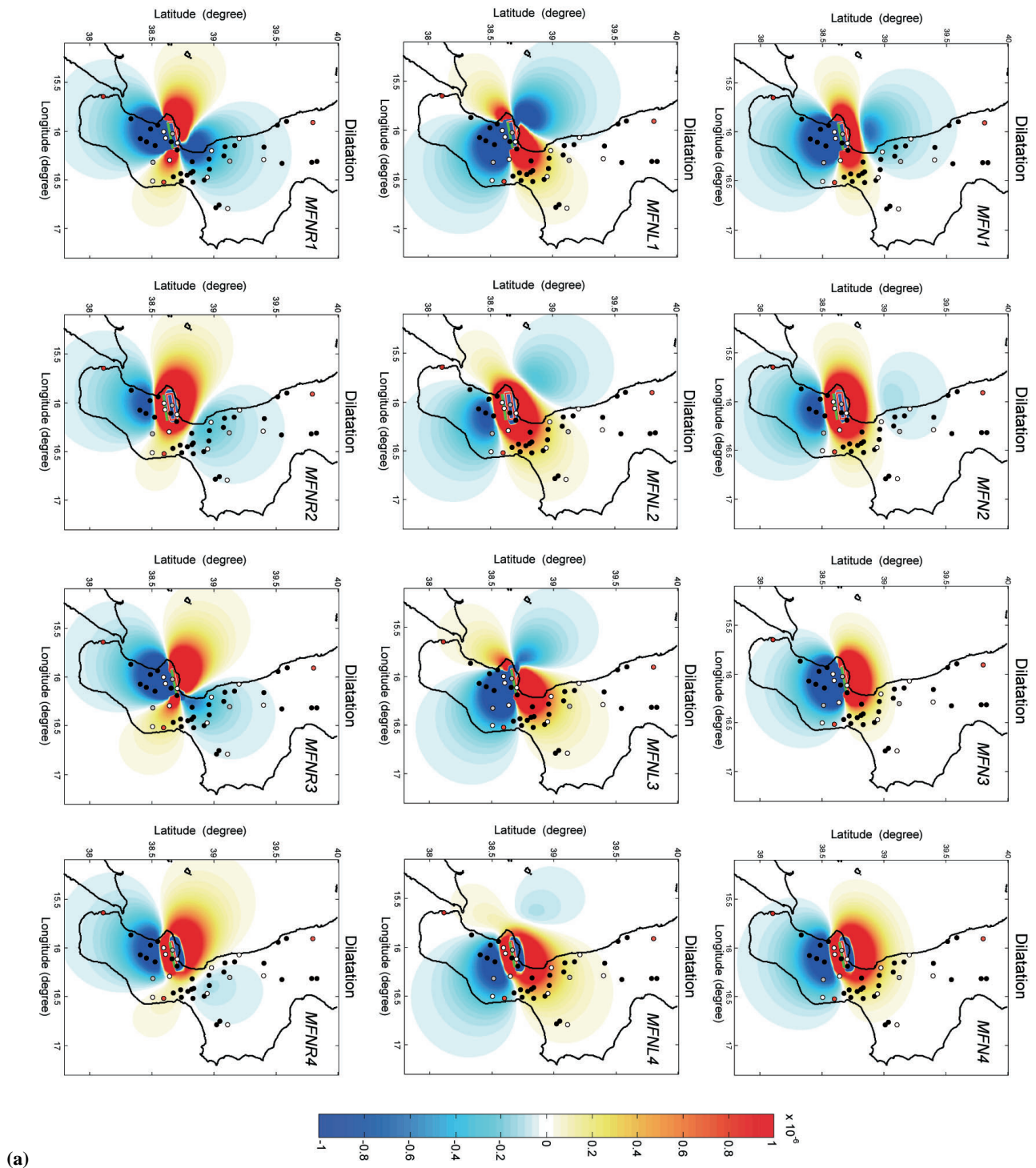
Macroseismic Fault North

(a)

Fig. 8. Comparison between calculated volumetric strain distributions and observed hydrological effects produced by the 1905 earthquake. Plots of surface static volumetric strain along five potential sources are calculated for different geometries and styles of faulting (the abbreviation of the individual fault is shown in the upper right side of each plot, refer to Table 3 for fault parameters); blue shading indicates areas in compression, red shading areas in dilatation. Units: 10^{-6}. A red rectangle indicates the surface projection of the fault plane; a green line is the intersection of the updip projection of the fault with the surface. Streamflow changes are indicated by circles (black/discharge increase; white/discharge decrease; grey/unspecified change; red/other effect). An increase of discharge is expected in compressional areas, a streamflow decrease in dilatational areas.
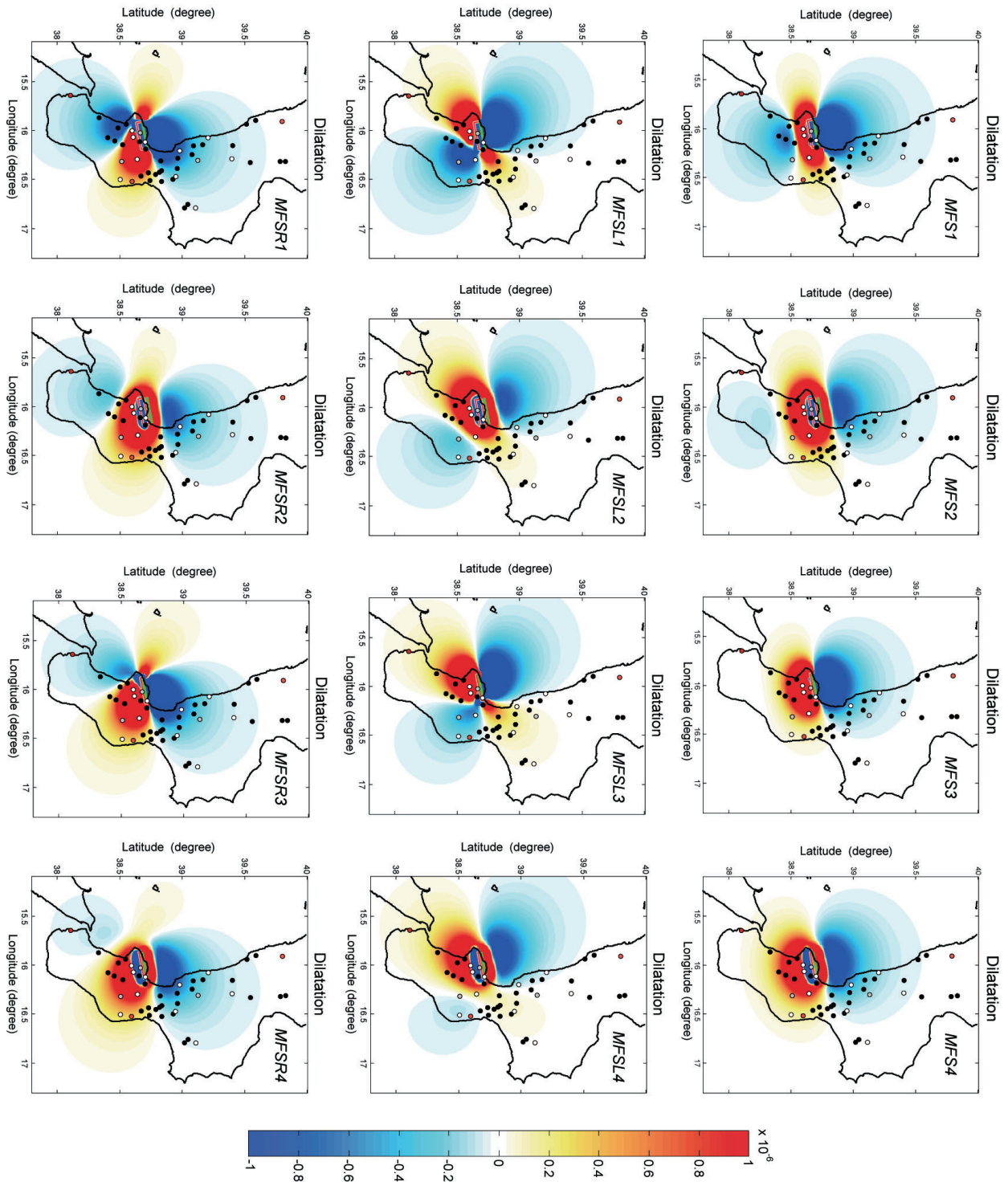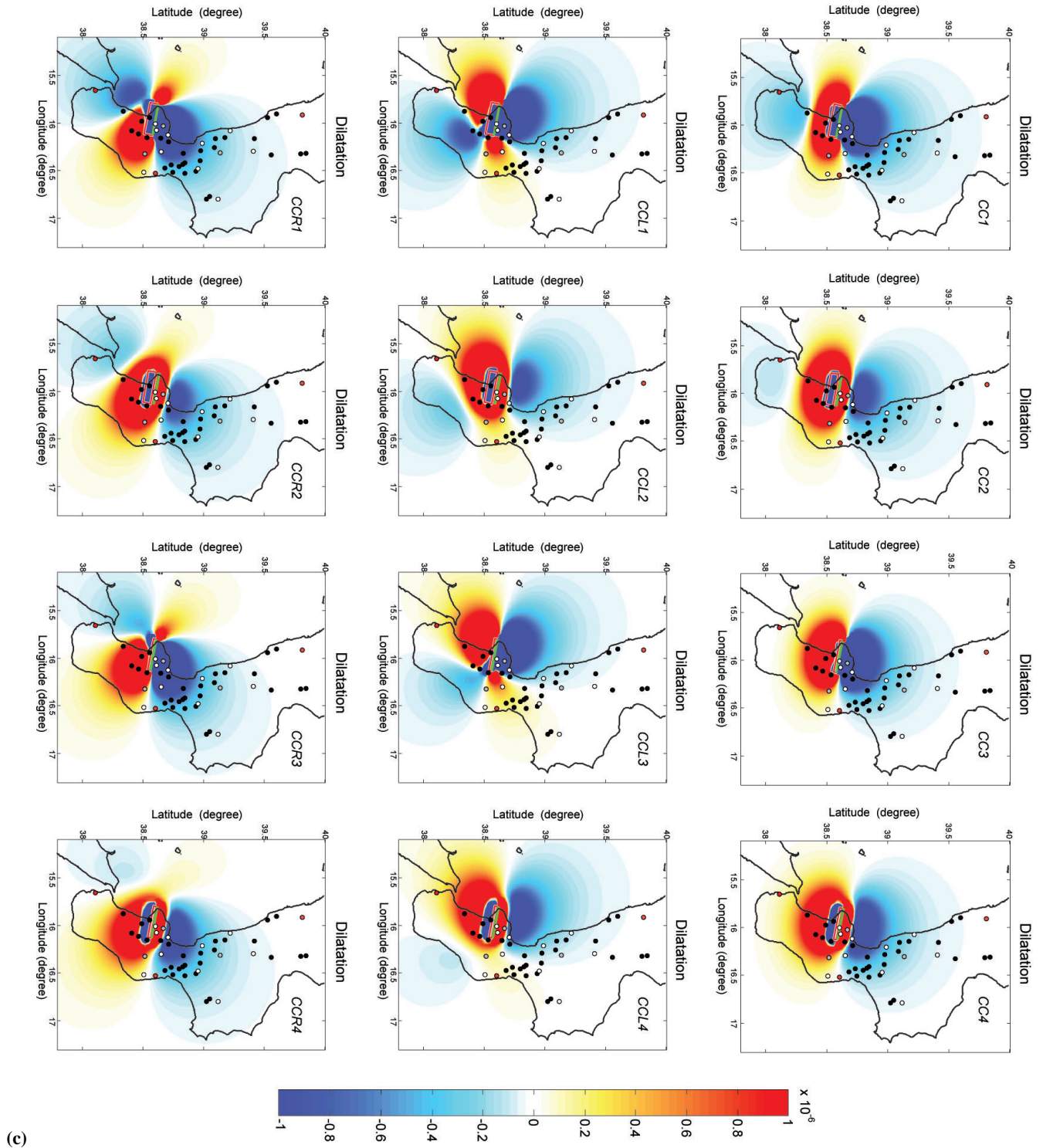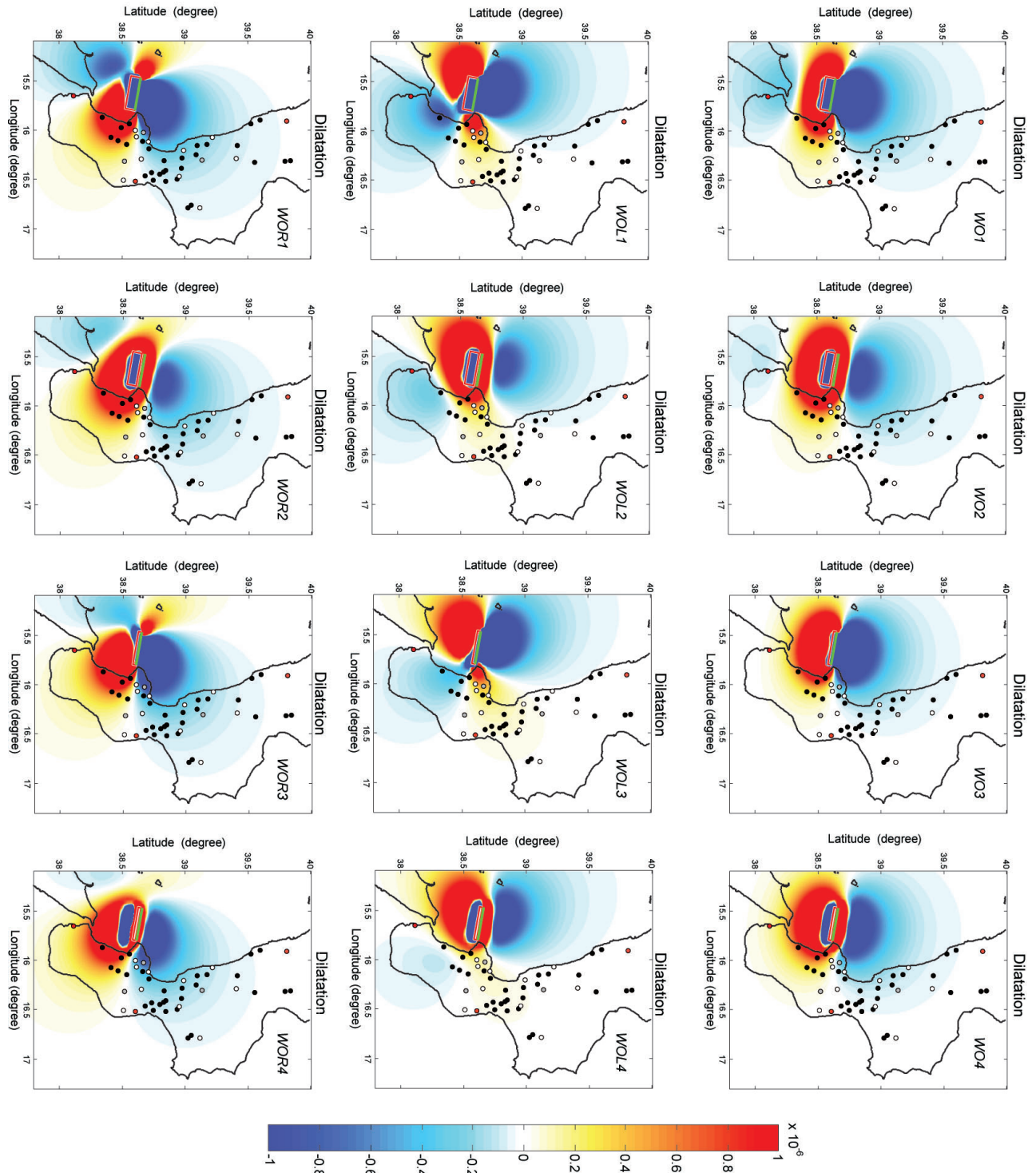
Macroseismic Fault South

(b)

Fig. 8. Continued.

Coccorino Fault
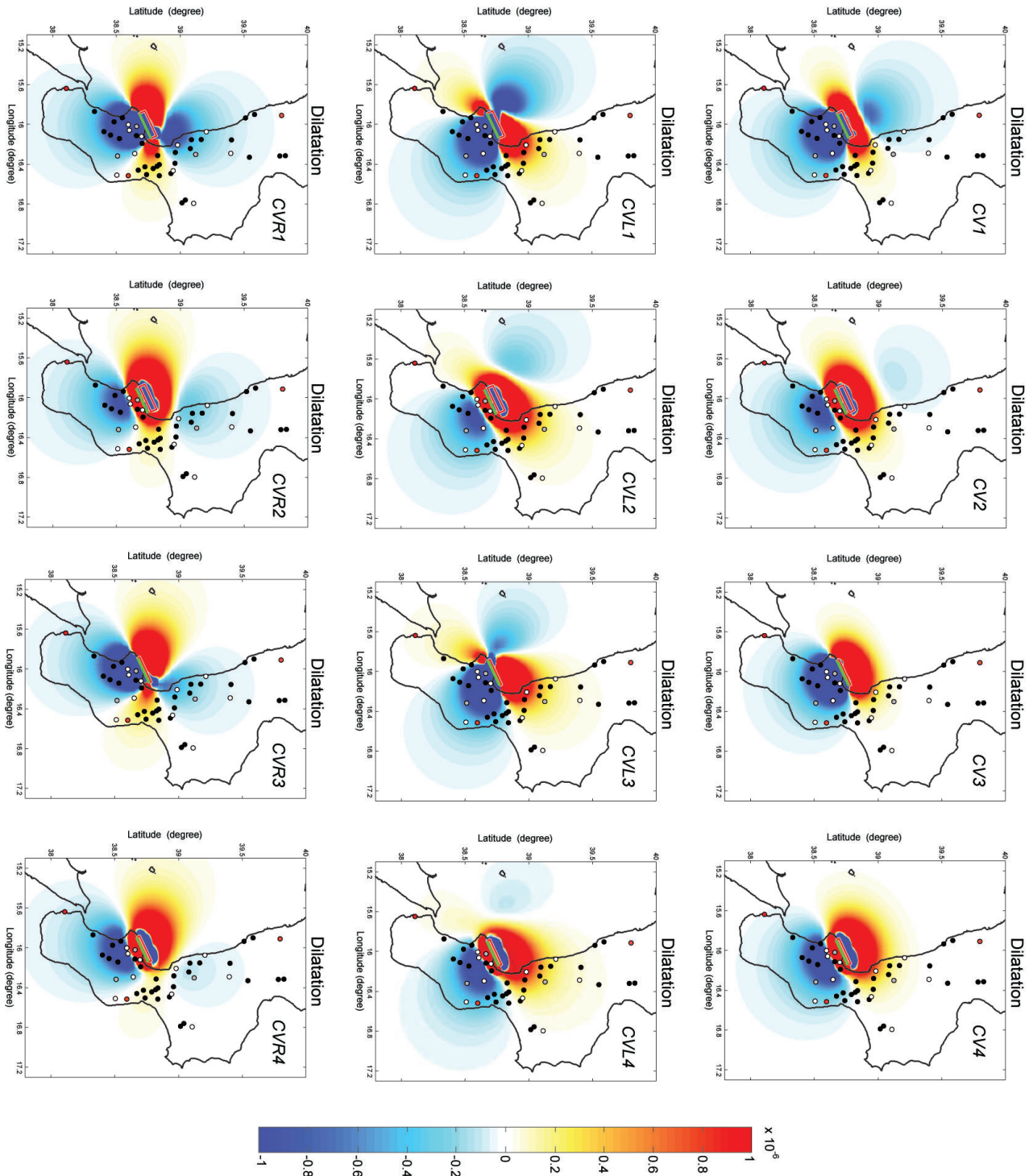

(c)

Fig. 8. Continued.

Western Offshore Fault

(d)

Fig. 8. Continued.

Capo Vaticano Fault

Fig. 8. Continued.

(e)

Table 3. Summary of the comparison between expected deformation and hydrological changes on the 60 individual fault.

		Rake (deg.)	270°	270°	270°	270°	309°	309°	309°	309°	231°	231°	231°	231°
		Dip (deg.)	60°	60°	80°	80°	60°	60°	80°	80°	60°	60°	80°	80°
		Top (km)	0	5	0	5	0	5	0	5	0	5	0	5
Fault	WO		WO1	WO2	WO3	WO4	WOL1	WOL2	WOL3	WOL4	WOR1	WOR2	WOR3	WOR4
	MFN		MFN1	MFN2	MFN3	MFN4	**MFNL1**	MFNL2	MFNL3	MFNL4	**MFNR1**	**MFNR2**	**MFNR3**	**MFNR4**
	MFS		**MFS1**	MFS2	MFS3	MFS4	MFSL1	MFSL2	MFSL3	MFSL4	**MFSR1**	MFSR2	MFSR3	MFSR4
	CV		CV1	CV2	CV3	CV4	CVL1	CVL2	CVL3	CVL4	CVR1	CVR2	CVR3	CVR4
	CC		CC1	**CC2**	CC3	**CC4**	CCL1	CCL2	CCL3	CCL4	CCR1	**CCR2**	CCR3	**CCR4**

Solutions like WOL1 satisfy both the condition 1 (within two-faults distance, more than 50% of points with polarities of the observed hydrological effects in agreement with the expected deformation) and the condition 2 (percentage of consistent polarities at one-fault distance higher than the percentage at two-faults distance). Solutions like **MFS1** satisfy only condition 1. Solutions like WO1 are discarded.

discharge) to the modeled coseismic static strain. Also in this case epicenter A showed a good agreement with the observed streamflow changes (Fig. 8d). On the contrary, poor fit was obtained for the epicenter C (Fig. 8e): we believe that this was the less probable location for the 1905 earthquake. Epicenter B showed a good agreement with the hydrological effects polarities, too (Fig. 8a and b); however, this localization displayed a higher uncertainty as it derived from the inversion of intensity data rather poorly distributed along the coastline. In addition, the $M=6.58$ mean magnitude from environmental effects associated with this location was slightly lower than the $M=6.7$ proposed magnitude. We conclude that A is the most constrained epicentral location of the 1905 event.

iii) Clues on geometry: the comparison of the observed hydrological changes with the expected coseismic static strain calculated on 60 individual faults allowed us to discard all the solutions with right-lateral component. On the contrary, two groups of faults were consistent with the polarities from the observations: the first belonged to a family of 100° oriented faults, (CC and WOL, Fig. 8c–d and Table 3), associated with the A offshore epicenter. All these faults displayed a component of left-lateral slip. The second belonged to a group of 260° oriented faults (one pure normal and two normal with left-lateral component solutions, MFN, Fig. 8a and Table 3) associated with the B inland epicenter. Furthermore, whilst the change of the fault dip did not visibly affect the pattern of expected strain, an important indication was that five preferred solutions out of seven derived from models of fault with depth of the top at 5 km; this is consistent with the generally accepted lack of any primary surface faulting produced by the event.

8 Conclusions

In this study, we significantly reduced the uncertainties concerning the size, location and geometry of the 1905 earthquake by using the environmental effects produced by the event. Summarizing our main conclusions in the light of the

above discussed issues, we associate all the observed environmental changes produced by the 1905 earthquake with a $M \geq 6.7$ event, most likely occurred in an offshore area west of Capo Vaticano (hence west of the location proposed by the historical seismic Catalogs) and possibly generated by a 100° N oriented normal fault with a left-lateral component. We support this characterization of the event source because: i) it shows the same minimum $M=6.7$, constantly obtained at location A from all the studied environmental effects; ii) it is highly consistent with the general pattern of the environmental effects observed following the earthquake (maximum distance landslides-epicenter, good fit between calculated strain and observed hydrological changes); iii) it is consistent with the lack of primary surface faulting associated with the event; iv) it may reasonably explain the moderate tsunami produced by the earthquake; v) it is consistent with the orientation of the extension acting in this area, which strikes NW-SE (Montone et al., 1999, 2004; see also inset in Fig. 1). In particular, a 100° N oriented normal fault with left-lateral component, located offshore nerby Capo Vaticano, could act as a regional transversal tectonic lineament that transfers the extensional deformation from the NE-trending structures in the Tyrrhenian northern offshore to the NE-trending faults that are reported inland, south of Capo Vaticano (Valensise and Pantosti, 2001; Galli and Bosi, 2002).

This paper shows the use of "macroscopic evidences", such as hydrological changes and ground failures, to infer the causative source of an earthquake. We suggest that the approach proposed provides tools to widen the knowledge of historical earthquakes for which instrumental data are contradictory or lacking, and to simulate the analysis of earthquakes occurred in non-urbanized areas.

References

Abe, K. and Noguchi, S.: Revision of magnitudes of large shallow earthquakes, 1897–1912, Phys. Earth Planet. In., 33, 1–11, 1983.

Almagià, R.: Studi geografici sulle frane in Italia, vol. II, L'Appennino centrale e meridionale. Conclusioni generali, Mem. Soc. Geogr. It., Roma, 14, 431 pp., 1910.

Annali dell' Ufficio di Metereologia e Geodinamica Italiano, Roma, serie II, Vol. 27, 1905 (parte I), 1908.

Argnani, A. and Trincardi, F: Paola slope basin: evidence of regional contraction of the eastern Tyrrhenian margin, Mem. Soc. Geol. It., 44, 93–105, 1988.

Baratta, M.: Il grande terremoto calabro dell'8 settembre 1905, Atti Soc. Toscana di Sc. Nat., XXII, 57–80, 1906.

Boschi E., Ferrari, G., Gasperini, P., Guidoboni, E., Smriglio, G., and Valensise, G.: Catalogo dei forti terremoti in Italia dal 461 a.C. al 1980, ING-SGA, Bologna, 1995.

Caporali, A., Braitenberg, C., and Massironi, M.: Geodetic and hydrological aspects of the Merano earthquake of 17 July 2001, J. Geodyn., 39, 17–336, 2005.

Chiodo, G., Dramis, F., Gervasi, A., Guerra, I., and Sorriso-Valvo, M.: Frane sismo-indotte e pericolosità di sito: primi risultati dello studio degli effetti di forti terremoti storici in Calabria centro-settentrionale, 18 GNGTS, Roma, 1999.

CPTI Working Group: Catalogo Parametrico dei Terremoti Italiani, vers. 2004 (CPTI04), INGV, Bologna, available at: http://emidius.mi.ingv.it/CPTI04/, 2004.

Cucci, L. and Tertulliani, A.: I terrazzi marini nell'area di Capo Vaticano (Arco Calabro): solo un record di sollevamento regionale o anche di deformazione cosismica?, Il Quaternario, 19, 89–101, 2006.

Duda, S. J.: Secular seismic energy release in the circum-Pacific belt, Tectonophysics, 2, 409–452, 1965.

Esposito, E., Porfido, S., Simonelli, A., Mastrolorenzo, G., and Iaccarino, G.: Landslides and other surface effects induced by the 1997 Umbria-Marche seismic sequence, Eng. Geol., 58, 353–376, 2000.

Fantucci, R. and Sorriso-Valvo, M.: Dendrogeomorphological analysis of a slope near Lago, Calabria (Italy), Geomorphology, 30, 165–174, 1999.

Galli, P.: New empirical relationships between magnitude and distance for liquefaction, Tectonophysics, 324, 169–187, 2000.

Galli, P. and Bosi, V.: Paleoseismology along the Cittanova fault: Implications for seismotectonics and earthquake recurrence in Calabria (Southern Italy), J. Geoph. Res., 107(B3), 2044, 10.1029/2001JB000234, 2002.

Gamberi, F. and Marani, M.: Downstream evolution of the Stromboli slope valley (southeastern Tyrrhenian Sea), Mar. Geol., 243, 180-199, 2007.

Gasperini, P., Bernardini, F., Valensise, G., and Boschi, E.: Defining seismogenic sources from historical earthquake felt reports, B. Seismol. Soc. Am., 89, 94–110, 1999.

Ge, S. and Stover, S. C.: Hydrodynamic response to strike- and dip-slip faulting in a half-space, J. Geophys. Res., 105(B11), 25513–25524, 2000.

Grecksch, G., Roth, F., and Kumpel, H. J.: Coseismic well-level changes due to the 1992 Roermond earthquake compared to static deformation of half-space solutions, Geophys. J. Int., 138, 470–478, 1999.

Harp, E. and Jibson, R. W.: Landslides triggered by the 1994 Northridge, California, earthquake, B. Seismol. Soc. Am., 86(1), 319–332, 1996.

Keefer, D. K.: Landslides caused by earthquakes, Geol. Soc. Am. Bull., 95, 406–421, 1984.

Keefer, D. K.: Statistical analysis of an earthquake-induced landslide distribution. The 1989 Loma Prieta, California event, Eng. Geol., 58, 231–249, 2000.

Kojima, H. and Obayashi, S.: An inverse analysis of unobserved trigger factor for slope stability evaluation, Comput. Geosci., 32, 1069–1078, 2006.

Lais, G.: Risultati preliminari di un'escursione in Calabria per lo studio dei fenomeni prodotti dalla commozione tellurica del 1905, Atti Pont. Acc. Rom. dei Nuovi Lincei, LIX, 77–85, 1906.

Lee, M., Liu, T. K., Ma, K. F., and Chang, Y. M.: Coseismic hydrological changes associated with dislocation of the September 21, 1999 Chichi earthquake, Taiwan, Geophys. Res. Lett., 29, 1824, doi:10.1029/2002GL015116, 2002.

Lin, J. and Stein, R. S.: Stress triggering in thrust and subduction earthquakes, and stress interactions between the southern San Andreas and nearby thrust and strike-slip faults, J. Geophys. Res., 109, B02303, doi:10.1029/2003JB002607, 2004.

Manga, M.: Origin of postseismic streamflow changes inferred from baseflow recession and magnitude-distance relations, Geophys. Res. Lett., 28, 2133–2136, 2001.

Martini, M. and Scarpa, R.: Earthquakes in Italy in the last century, in: Earthquakes, Observation Theory and Interpretation, edited by: Kanamori, H. and Boschi, E., 85th E. Fermi Summer School in Geophysics, North Holland Publ. Co., 479–492, 1983.

Mercalli, G.: Alcuni risultati ottenuti dallo studio del terremoto calabrese dell' 8 settembre 1905, Atti Acc. Pontoniana di Napoli, XXXVI, Mem. 8, 1–9, 1906.

Michelini, A., Lomax, A., Nardi, A., and Rossi A.: La localizzazione del terremoto della Calabria dell'8 settembre 1905 da dati strumentali, in: 8 settembre 1905, terremoto in Calabria, edited by: Guerra, I. and Savaglio, A., Università della Calabria, 225–240, 2006.

Montanari, G.: Studio generale dei movimenti franosi in provincia di Catanzaro, Ann. Lavori Pubblici, anno LXXVIII, 3, 125.231, 1940.

Montgomery, D. R. and Manga, M.: Streamflow and water well responses to earthquakes, Science, 300, 2047–2049, 2003.

Montgomery, D. R., Greenberg, H. M., and Smith, D. T.: Streamflow responses to the Nisqually earthquake, Earth Planet. Sc. Lett., 209, 19–28, 2003.

Montone, P., Amato, A., and Pondrelli, S.: Active stress map of Italy, J. Geophys. Res., 104(B11), 25595–25610, 1999.

Montone, P., Mariucci, M. T., Pondrelli, S., and Amato, A.: An improved stress map for Italy and surrounding regions (central Mediterranean), J. Geophys. Res., 109, B10410, doi:10.1029/2003JB002703, 2004.

Muir-Wood, R. and King, C. P.: Hydrological signatures of earthquake strain, J. Geophys. Res., 98, 22035–22068, 1993.

Mulargia, F., Baldi, P., Achilli, V., and Broccio, F.: Recent crustal deformations and tectonics of the Messina Strait area, Geophys. J. Roy. Astr. S., 76, 369–381, 1984.

Neri, G., Barberi, G., Orecchio, B., and Mostaccio, A.: Seismic strain and seismogenic stress regimes in the crust of the southern Tyrrhenian region, Earth Planet. Sc. Lett., 213, 97-112, 2003.

Okada, Y.: Internal deformation due to shear and tensile faults in a half-space, B. Seismol. Soc. Am., 82, 1018–1040, 1992.

Piatanesi, A. and Tinti, S.: Numerical modelling of the 8 September 1905 Calabrian (Southern Italy) tsunami, Geophys. J. Int., 150, 271–284, 2002.

Pizzino, L., Burrato, P., Quattrocchi, F., and Valensise, G.: Geochemical signatures of large active faults: The example of the 5 February 1783, Calabrian earthquake (southern Italy), J. Seismol., 8, 363–380, doi:10.1023/B:JOSE.0000038455.56343.e7, 2004.

Porfido, S., Esposito, E., Vittori, E., Tranfaglia, G., Michetti, A. M., Blumetti, M., Ferreli, L., Guerrieri, L., and Serva, L.: Areal distribution of ground effects induced by strong earthquakes in the Southern Apennines (Italy), Surv. Geophys., 23, 529–562, 2002.

Postpischl, D. (Ed.): Catalogo dei terremoti italiani dall'anno 1000 al 1980, Consiglio Nazionale delle Ricerche, Progetto Finalizzato Geodinamica (CNR-PFG), Quaderni de "La Ricerca Scientifica", Bologna, 1145, 2b, 239 pp., 1985.

Prestininzi, A. and Romeo, R.: Earthquake-induced ground failures in Italy, Eng. Geol., 58, 387–397, 2000.

Riuscetti, M. and Schick, R.: Earthquakes and tectonics in Southern Italy, Proceedings of Joint Symposium of the European Seismological Commission and the European Geophysical Society, Trieste, 59–78, 21 September 1974.

Rizzo, G. B.: Contributo allo studio del terremoto della Calabria del giorno 8 settembre 1905, Atti R. Acc. Peloritana, XXII, fasc. I, 2–87, 1907.

Rodriguez, C. E., Bommer, J. J., Chandler, R. J.: Earthquake-induced landslides, 1980–1997, Soil Dyn. Earthq. Eng., 18, 325–346, 1999.

Tinti, S., Maramai, A. and Graziani, L.: The new catalogue of Italian tsunamis, Nat. Hazards, 33, 439–465, 2004.

Toda, S., Stein, R. S., Richards-Dinger, K., and Bozkurt, S.: Forecasting the evolution of seismicity in Southern California: Animation in building stress transfer, J. Geophys. Res., 110, B05S16, doi:10.1029/2004JB003415, 2005.

Tortorici, G., Bianca, M., De Guidi, G., Monaco, C., and Tortorici, L.: Fault activity and marine terracing in the Capo Vaticano area (southern Calabria) during the Middle-Late Quaternary, Quatern. Int., 101–102, 269–278, 2003.

Trincardi, F., Cipolli, M., Ferretti, P., La Morgia, J., Ligi, M., Marozzi, G., Palumbo, V., Taviani, M., and Zitellini, N.: Slope basin evolution on the Eastern Tyrrhenian margin: preliminary report, Giornale di Geologia, 49/2, 1–9, 1987.

Valensise, G. and Pantosti, D. (Eds.): Database of potential sources for earthquakes larger than M 5.5 in Italy, Ann. Geofis., Supplement to vol. 44(4), 180 pp., 2001.

Wells, D. L. and Coppersmith, K. J.: New empirical relationships among magnitude, rupture length, rupture width, rupture area, and surface displacement, B. Seismol. Soc. Am., 84, 974–1002, 1994.

Westaway, R.: Seismic moment summation for historical earthquakes in Italy: tectonic implications, J. Geophys. Res., 97, 15437–15464, 1992.